# Real-time monitoring of Ti(IV) metal ion binding of transferrin using a solid-state nanopore *⊙*

**Special Collection: Polymer Nanoconfinement** 

Matthew O'Donohue <sup>(i)</sup>; Madhav L. Ghimire <sup>(i)</sup>; Sangyoup Lee <sup>(i)</sup>; Min Jun Kim **□** 



J. Chem. Phys. 160, 044906 (2024) https://doi.org/10.1063/5.0185590







**The Journal of Chemical Physics** 

Special Topic: Molecular Dynamics, Methods and Applications 60 Years after Rahman

**Submit Today** 





# Real-time monitoring of Ti(IV) metal ion binding of transferrin using a solid-state nanopore

Cite as: J. Chem. Phys. 160, 044906 (2024); doi: 10.1063/5.0185590 Submitted: 31 October 2023 • Accepted: 2 January 2024 •







Matthew O'Donohue, 1 D Madhav L. Ghimire, 2 D Sangyoup Lee, 3 D and Min Jun Kim<sup>1,2,a)</sup> D



Published Online: 26 January 2024









### **AFFILIATIONS**

- Applied Science Program, Southern Methodist University, Dallas, Texas 75205, USA
- <sup>2</sup>Department of Mechanical Engineering, Southern Methodist University, 3101 Dyer Street, Dallas, Texas 75205, USA
- <sup>3</sup>Bionic Research Center, Biomedical Research Division, Korea Institute of Science and Technology, Seoul, Republic of Korea

Note: This paper is part of the JCP Special Topic on Polymer Nanoconfinement.

a) Author to whom correspondence should be addressed: mjkim@lyle.smu.edu

#### **ABSTRACT**

Transferrin, a central player in iron transport, has been recognized not only for its role in binding iron but also for its interaction with other metals, including titanium. This study employs solid-state nanopores to investigate the binding of titanium ions [Ti(IV)] to transferrin in a single-molecule and label-free manner. We demonstrate the novel application of solid-state nanopores for singlemolecule discrimination between apo-transferrin (metal-free) and Ti(IV)-transferrin. Despite their similar sizes, Ti(IV)-transferrin exhibits a reduced current drop, attributed to differences in translocation times and filter characteristics. Single-molecule analysis reveals Ti(IV)transferrin's enhanced stability and faster translocations due to its distinct conformational flexibility compared to apo-transferrin. Furthermore, our study showcases solid-state nanopores as real-time monitors of biochemical reactions, tracking the gradual conversion of apo-transferrin to Ti(IV)-transferrin upon the addition of titanium citrate. This work offers insights into Ti(IV) binding to transferrin, promising applications for single-molecule analysis and expanding our comprehension of metal-protein interactions at the molecular

Published under an exclusive license by AIP Publishing. https://doi.org/10.1063/5.0185590

### I. INTRODUCTION

Iron holds a central role in health and disease in the human body, 1-3 with its presence enabling hemoglobin synthesis 4 and its absence causing diseases such as anemia. As such, elaborate systems have been developed in mammals for the procurement and distribution of iron.<sup>5</sup> Toward this end, vertebrates developed an ~80 kDa glycoprotein called transferrin. 6-8 Transferrin is the major iron transporter in the blood and has two binding domains that reversibly bind iron ions with high affinity (log K = 22.5 and 21.4). However, transferrin in the blood is only 30% saturated with iron on average, 11 causing researchers to question whether transferrin also binds other metal ions. Indeed, transferrin has been shown to bind titanium,<sup>12</sup> vanadium,<sup>13</sup> and chromium,<sup>14</sup> among other metals.<sup>15</sup> Of particular importance is transferrin's ability to bind to titanium ions, as it is involved in the bioactivity of Ti-containing anticancer drugs<sup>12,16</sup> and in binding titanium ions released from implants.

The titanium ion [Ti(IV)] is similar in size to the iron ion [Fe(III)], but it is a stronger Lewis acid. 17,18 Indeed, transferrin was shown to bind Ti(IV) more tightly than Fe(III). Tinoco and Valentine were the first to demonstrate that Ti(IV) binds more tightly to transferrin by using UV/vis kinetics and isothermal titration calorimetry. Tinoco and Valentine showed that Ti(IV) binds to one of transferrin's binding sites more tightly than the other. Here, we use a solid-state nanopore (SSN) to probe transferrin's affinity for Ti(IV) and classify Ti(IV)-bound transferrin in a single-molecule and label-free manner.

SSNs are an attractive tool for single-molecule studies of biomolecules.<sup>19</sup> Nanopores have extensively been used to probe and have been shown to be sensitive enough to differentiate proteins that differ in a single amino acid<sup>23</sup> or in their post-translational modifications.<sup>24</sup> An SSN measures the modulation of ionic current through a nanoscopic opening that separates two chambers [Fig. 1(c)]. Both cis and trans chambers are filled with an electrolytic solution, and an electrode is placed into each chamber. A voltage bias is applied at the electrodes, and the majority of the electric potential drop occurs across the nanopore that separates the two chambers. When a molecule traverses the nanopore, it causes a

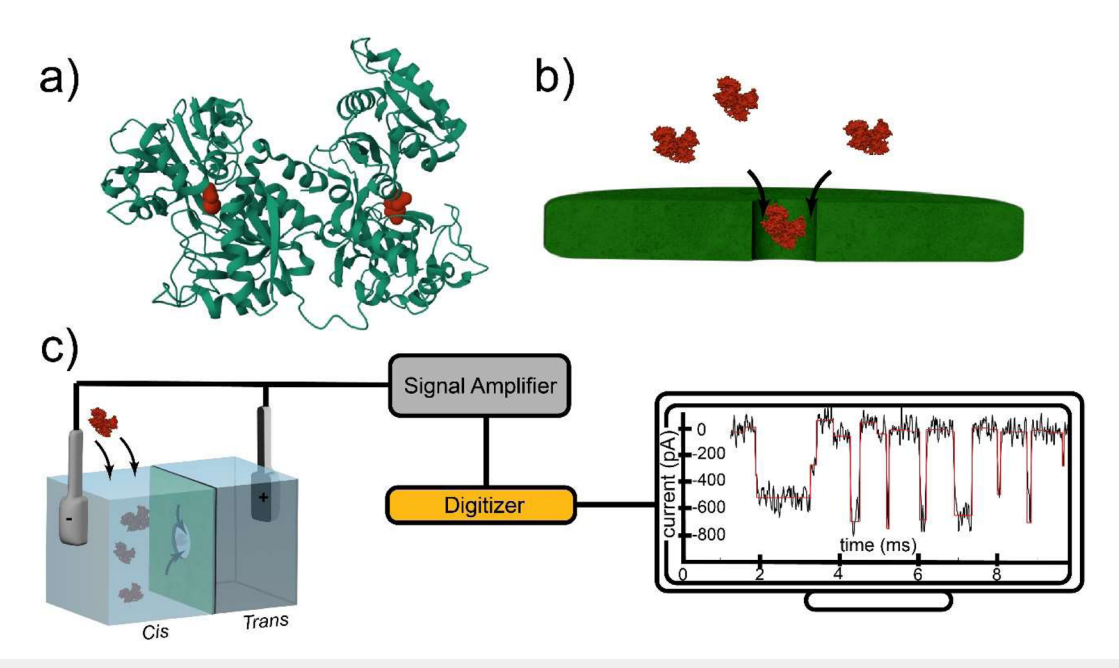


**FIG. 1.** (a) 3D structure of titanium-bound human serum transferrin protein. Transferrin is an  $\sim$ 80 kDa protein that consists of 679 amino acids. The red globules represent the locations where titanium ions bind to transferrin. (b) In nanopore experiments, proteins are driven across a nanometer-sized pore through electrophoresis or electro-osmosis. (c) Basic nanopore setup: Both the cis and trans reservoirs are filled with an electrolyte solution. Protein is added to the cis chamber, and an external voltage is applied to drive the proteins through the nanopore. The signal is then amplified, digitized, and processed on a computer.

distinctive resistive pulse in the measured electronic current, defined by its translocation time ( $\Delta t$ ) and current drop ( $\Delta I$ ). Nanopores made with solid-state materials have extensively been developed and used to characterize proteins. <sup>19,21,25–31</sup>

Here, we show that an SSN can be used to distinguish between Ti(IV)-bound transferrin and transferrin without any metal ions bound (called apo-transferrin) on a single molecule basis. Furthermore, we find that the binding of Ti(IV) to transferrin causes transferrin to adopt a more compact and stable conformation that causes transferrin to transit the nanopore more quickly than when it is not bound to any metal ions. Finally, we show that an SSN can be used as a real-time monitor of the reaction progress as transferrin binds to Ti(IV) ions.

### **II. MATERIALS AND METHODS**

### A. Nanopore fabrication

All nanopores were fabricated using a  $12 \pm 2$  nm thick silicon nitride membrane (Norcada Inc., NXDB-50H105V122) through the well-established chemically tuned dielectric breakdown method (CT-CDB). <sup>32,53</sup> The diameter of all nanopores used in experiments was  $19 \pm 1$  nm. This diameter was chosen because it maintained a sufficiently high signal-to-noise ratio (SNR), while minimizing protein clogging in the nanopore. To fabricate the nanopore, we placed two polydimethylsiloxane (PDMS) gaskets on each side of the silicon nitride membrane, which was then sandwiched between two Teflon flow cells [see Fig. 1(c)]. During fabrication, the reservoirs of the flow cells were filled with 1M KCl at pH 8, and sodium hypochlorite was added to each reservoir at a volumetric ratio of 2:9. <sup>34</sup> Ag/AgCl

electrodes were placed in each reservoir, and a custom-built circuit was used to apply a voltage sufficient to cause pore formation in the membrane.<sup>21</sup> Pore formation is indicated by a sudden spike in ionic current, representing the increased ionic flow across the membrane due to the nanopore being formed. The conductance across the nanopore was measured and related to the diameter of the nanopore using the following equation:

$$G = \sigma \left[ \frac{4L}{\pi D^2} + \frac{1}{D} \right]^{-1},\tag{1}$$

where  $\sigma$ , L, and D are the conductivity of the electrolyte solution, nominal thickness of the nanopore, and nanopore diameter, respectively. The initial pore was formed, we applied short voltage pulses to increase its diameter to the desired size. An IV plot was measured for all pores and confirmed to be ohmic before conducting experiments (refer to Figs. S1–S4 of the supplementary material). The 1M KCl solution used during the CT-CDB process was then removed, and the reservoirs were thoroughly washed with copious amounts of water, followed by ethanol. Once cleaned, the reservoirs were filled with the electrolyte solution used during experiments. Baseline measurements were performed to ensure the absence of events and to verify the pore size remained stable.

# B. Protein preparation and addition for nanopore experiments

Apo-transferrin (transferrin with no metal ions bound to it) was purchased from Sigma-Aldrich (product number T1147) and reconstituted in 1X Phosphate Buffered Saline (PBS). Titanium-

bound transferrin was obtained as described in Sec. II C. All proteins used were dialyzed extensively against the solution used during the nanopore experiments before conducting the experiments. In the nanopore experiments, protein was added to the cis-side reservoir of the flow cell at a concentration of 100 nM.

### C. Binding of Ti(IV) to transferrin

Transferrin was bound to Ti(IV) following the procedure described by Tinoco and Valentine. Titanium must be bound to an anionic ligand—in this case, citrate—for transferrin binding to occur. To briefly summarize, Na<sub>8</sub>[Ti(C<sub>6</sub>H<sub>4</sub>O<sub>7</sub>)<sub>3</sub>]·17H<sub>2</sub>O was prepared by adding sodium citrate to TiCl<sub>3</sub>. The solution was airoxidized until it became clear, indicating that titanium had oxidized to Ti(IV). At this point, the Ti(IV) citrate species was ready for binding by transferrin. The Ti(IV) citrate species was added in excess (>800  $\mu$ M, as discussed in Sec. III) and allowed to react with 25  $\mu$ M of transferrin in a solution containing 10 mM sodium citrate, 20 mM NaHCO<sub>3</sub>, and 200 mM KCl at pH 7.4. The binding of Ti(IV) to transferrin was confirmed by monitoring UV/vis at 321 nm. The resulting solution was then extensively dialyzed (20 kDa Slide-A-Lyzer, Thermo Fisher) to remove the excess Ti(IV) citrate species.

# D. UV/vis spectroscopy of Ti(IV)-free transferrin and Ti(IV)-bound transferrin

The reaction of apo-transferrin with Ti(IV) was monitored using a UV/vis spectrometer (BioTek Epoch 2). The absorbance of the charge transfer band (300–500 nm) was monitored at regular time intervals. In particular, a shoulder was noticed around 321 nm, indicative of transferrin binding to Ti(IV).

### E. Electrical sensing for nanopore experimentation and analysis

An Axopatch 200B amplifier was used for signal acquisition in all nanopore experiments, and the signals were subsequently digitized using a Digidata 1550B device (Molecular Devices). During experiments, the raw signal was filtered using either a 10 kHz or a 100 kHz low-pass Bessel filter. Data were digitized using a sample rate of 250 kHz. The resistive pulses from protein translocations were analyzed using EventPro 3.0.<sup>38</sup> A custom MATLAB script was then employed to further analyze the data extracted from EventPro 3.0.

#### III. RESULTS AND DISCUSSION

### A. Using a nanopore to discriminate between titanium-bound and titanium-free transferrin

When transferrin is not bound to any metal ions, it is referred to as *apo-transferrin*, with a molecular weight of ~80 kDa. When transferrin is bound to two titanium ions, it is known as Ti(IV)-transferrin. The weight of Ti(IV)-transferrin is roughly the same as apo-transferrin since the two titanium ions have a negligible impact on the protein's weight. However, Ti(IV)-transferrin adopts a more stable conformation than apo-transferrin. This difference in conformation can be exploited by a nanopore to distinguish between the two. In Fig. 2(a), we compare the relative current drop ( $\Delta I/I$ ) histograms of apo-transferrin and Ti(IV)-transferrin at 2M KCl. As observed, apo-transferrin consistently exhibits a greater current drop than Ti(IV)-transferrin, similar to what was observed in Saharia *et al.*, where iron-bound transferrin had a lower peak current drop than apo-transferrin. Fino-bound transferrin is

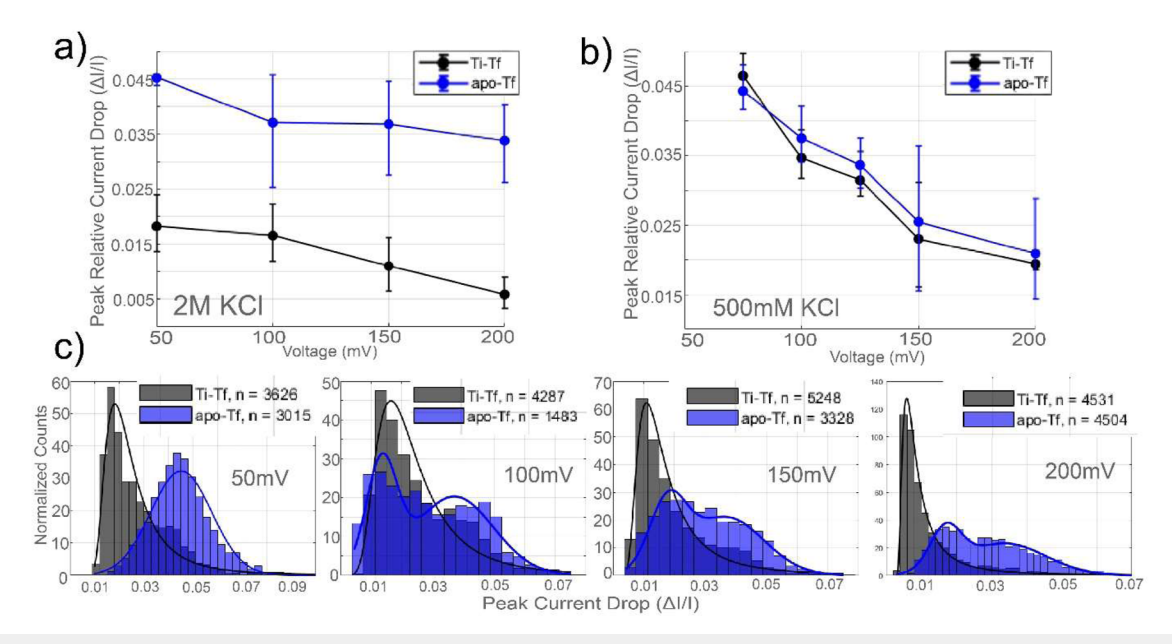


FIG. 2. Difference in the peak values of the relative current drop for apo-transferrin (apo-Tf) and Ti(IV)-bound transferrin (Ti-Tf) at (a) 2M KCl and (b) 500 mM KCl. (c) Histograms of the relative current drop (ΔI/I) of apo-transferrin and Ti(IV)-bound transferrin at 2M KCl for varying voltages. All error bars represent the bootstrapped confidence interval estimations of the medians.

similar to titanium-bound transferrin, with the difference being that transferrin binds titanium more tightly than it binds iron. In addition, transferrin adopts a more negative charge when bound to titanium ions (Secs. S1-S7 of the supplementary material). In conventional nanopore experiments, the larger size of a protein leads to a more significant exclusion of the electrolyte solution from the nanopore, resulting in a more pronounced decrease in current. This phenomenon is typically attributed to the excluded volume of the electrolyte.<sup>39</sup> However, as shown in Fig. 2(a), the opposite occurs: the marginally larger protein [Ti(IV)-transferrin)] has a lower current drop than the smaller protein (apo-transferrin). Apo-transferrin is partially unfolded, while Ti(IV)-transferrin adopts a more folded conformation. In their folded state, globular proteins typically have buried waters and internal cavities, which give them a larger molecular volume than when unfolded. 40 Thus, the difference in the current drop between apo-transferrin and Ti(IV)-transferrin cannot be explained by their differing molecular volumes. While current drop generally scales with molecular volume ( $\frac{\Delta I}{I} \propto \text{volume}$ ), it has also been reported that the amplitude of the current drop depends on other factors, such as the shape of the analyte. 46-49 As discussed in Sec. III B, the difference in the relative current drop between apo-transferrin and Ti(IV)-transferrin can be explained by their differing translocation times and the rise time of the Bessel filter used during experiments. The differing translocation times arise from conformational differences and differences in charge between apotransferrin and Ti(IV)-transferrin. Regardless of the origin of their differing resistive pulses, such experiments demonstrate that a solidstate nanopore can be used to discriminate between apo-transferrin and Ti(IV)-transferrin on a single-molecule basis.

The velocity of a particle under an applied voltage can be approximated as

$$v = \mu * E, \tag{2}$$

where E is the electric field strength and  $\mu$  is the electrophoretic mobility. The electrophoretic mobility is given by the following equation:

$$\mu = \frac{\varepsilon * \zeta * \eta}{\varepsilon_0},\tag{3}$$

where  $\mu$  is the electrophoretic mobility,  $\zeta$  is the zeta potential,  $\eta$  is the viscosity,  $\epsilon$  is the dielectric constant of the medium, and  $\epsilon_0$  is the permittivity of free space. Thus, a relative increase in the zeta potential (charge) of the protein is expected to result in a faster translocation time. We measured the zeta potential of apo-transferrin and Ti(IV)-transferrin (Table S1 of the supplementary material). As expected, the Ti(IV)-transferrin (metal-bound) assumed a more negative charge than the apo-transferrin. Since the titanium-bound transferrin has a more negative charge than the apo-transferrin at pH 7.4 (the pH used during experiments), it is expected that the titanium-bound transferrin will travel faster when subjected to an electrophoretic force than metal-free transferrin.

### B. Single-molecule evidence that titanium-bound transferrin is more stable than apo-transferrin

The translocation times of apo-transferrin and Ti(IV)transferrin through a nanopore were compared. As shown in Fig. 3(a), apo-transferrin consistently exhibited a greater median translocation time than Ti(IV)-transferrin. The median was chosen as the metric for comparing translocation times because it is less affected by outliers compared to the mean. The mean translocation times can be found in Secs. S1-S8 of the supplementary material and exhibited the same trend as the median translocation times. Figure 3(c) clearly demonstrates that the apo-transferrin exhibits a much wider range of translocation times than the Ti(IV)-transferrin. When transferrin binds a metal ion, it adopts a fully folded conformation. In the absence of a metal ion (apo-transferrin), transferrin remains partially unfolded. This unfolded state increases entropy by providing more conformational degrees of freedom for the protein. 41 In other words, apo-transferrin can assume a broader range of intermediate conformations. Consequently, it is more likely that apo-transferrin will temporarily interact with the silicon nitride surface of the nanopore due to these transient conformations. These evanescent interactions result in an extended translocation time for apo-transferrin.

The experiments shown in Fig. 3(a) were conducted in 2M KCl. Using a high salt concentration enhances the nanopore's capability to differentiate between similar proteins, but it comes at the cost of rapid protein translocation times. 42 The filter employed in our nanopore experiments was a 10 kHz Bessel filter. For Bessel filters, it is widely known that resistive pulses with durations faster than

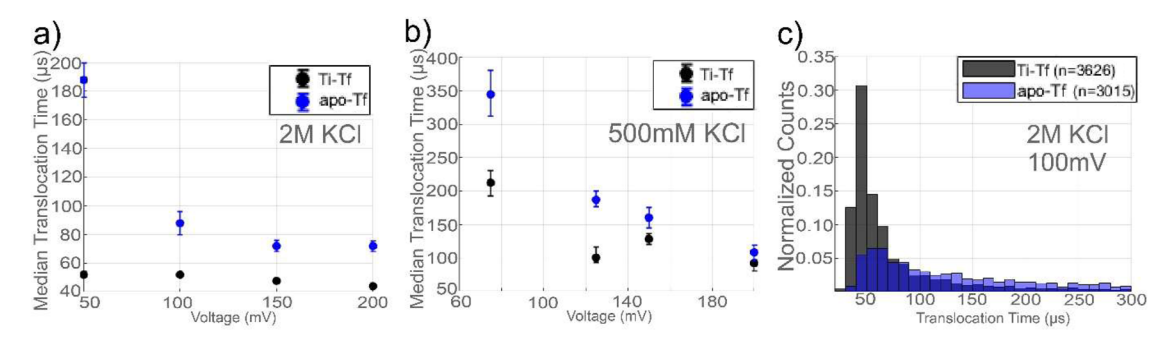


FIG. 3. Comparison of the median translocation times of apo-transferrin (apo-Tf) and Ti(IV)-bound transferrin (Ti-Tf) at (a) 2M KCl and (b) 500 mM KCl. (c) Exemplary translocation time histogram comparison of apo-transferrin and Ti(IV)-transferrin at 100 mV. The error bars represent the bootstrapped confidence intervals on the medians.

 $2 * t_r$  will not reach their full amplitude, where  $t_r$  represents the rise time of the filter. <sup>43,44</sup> In the case of 10 kHz filters,  $2 * t_r$  equals 70  $\mu$ s. Therefore, any event faster than 70  $\mu$ s will be attenuated, resulting in a smaller  $\Delta I$ . As observed in Fig. 3(a), apo-transferrin exhibits a translocation time greater than 70  $\mu$ s, whereas Ti(IV)-transferrin demonstrates translocation times that are significantly lower than 70 µs at all applied voltages. Consequently, the reduced current drop values ( $\Delta I$ ) for Ti(IV)-transferrin [see Fig. 2(c)] are likely artifacts caused by the severe attenuation of its signal due to its swift translocation. To verify this and further compare apo- and Ti(IV)transferrin, we conducted two additional sets of experiments. First, we compared the two proteins in a salt concentration of 500 mM KCl [Fig. 2(b)]. At this salt concentration, translocations were notably slower [see Fig. 3(b)] and well above the rise time attenuation threshold. Such a phenomenon has previously been observed in nanopores, where dendrimers traveled ~2× slower in 500 mM KCl than they did at 1M KCl.<sup>47</sup> When apo-transferrin and Ti(IV)-transferrin are compared in 500 mM KCl, their associated relative current drop histograms are much more similar to each other [see Fig. 2(b)] than when 2M KCl is used. There are two possible explanations for the observed similarities between apo-transferrin and Ti(IV)-transferrin at 500 mM KCl: (1) Apo-transferrin and Ti(IV)-transferrin have similar excluded volumes, and the differences shown in Fig. 2(a) are due to the attenuation of Ti(IV)-transferrin's signal caused by its rapid translocation time. (2) Apo-transferrin and Ti(IV)-transferrin have different excluded volumes, but the nanopore's sensitivity at 500 mM KCl is insufficient to differentiate between them. To determine which explanation is correct, we conducted the experiments again in 2M KCl, this time using a 100 kHz low-pass Bessel filter. The 100 kHz filter ensures that none of the rapid translocations are attenuated, and the signal-to-noise ratio (SNR) in 2M KCl was sufficiently high, eliminating concerns about noise at 100 kHz, masking any translocations (see S16 of the supplementary material). With the 100 kHz filter, apo-transferrin and Ti(IV)-transferrin exhibited

nearly identical peak current drop values from 50 to 100 mV (see Secs. S1 and S2 of the supplementary material). These experiments confirmed that the differences in resistive pulse values between apo- and Ti(IV)-transferrin at 2M KCl [Fig. 2(a)] were, indeed, a result of the attenuation of Ti(IV)-transferrin's resistive pulse signal due to its rapid translocation time. It is only when the voltage is increased beyond 150 mV that the two proteins become significantly distinguishable from each other. This is likely due to the voltage-induced unfolding of the proteins;<sup>45</sup> as the voltage increases, apo-transferrin becomes increasingly more unfolded, and thus, the likelihood of transient interactions with the pore wall also increases. As a control, we also analyzed the iron-bound transferrin, known as holo-transferrin. Holo-transferrin had nearly identical translocation times and current drop values as Ti(IV)-transferrin (see Fig. S7 of the supplementary material). This was expected, as both forms are stable, unlike apo-transferrin. In addition, both iron and titanium ions bind to the same site in transferrin.

### C. Real-time monitoring of titanium ion binding to transferrin

We explored the possibility of leveraging differences in translocation times between apo-transferrin and Ti(IV)-transferrin to use a nanopore as a real-time monitor of the conversion of apo-transferrin to Ti(IV)-transferrin. Initially, we introduced apo-transferrin into the cis chamber of the flow cell and allowed for over 1000 translocations to occur. Subsequently, we added an excess of titanium citrate to the cis side containing the apo-transferrin. The citrate functions as the anionic ligand in the coordination bond between transferrin and titanium. Figures 4(a) and 4(b) depict the change in the median translocation time following the addition of an excess of titanium citrate in 1X PBS and 2M KCl, respectively. As observed, the median translocation time decreases with increasing time, indicating the gradual conversion of apo-transferrin to Ti(IV)-transferrin.

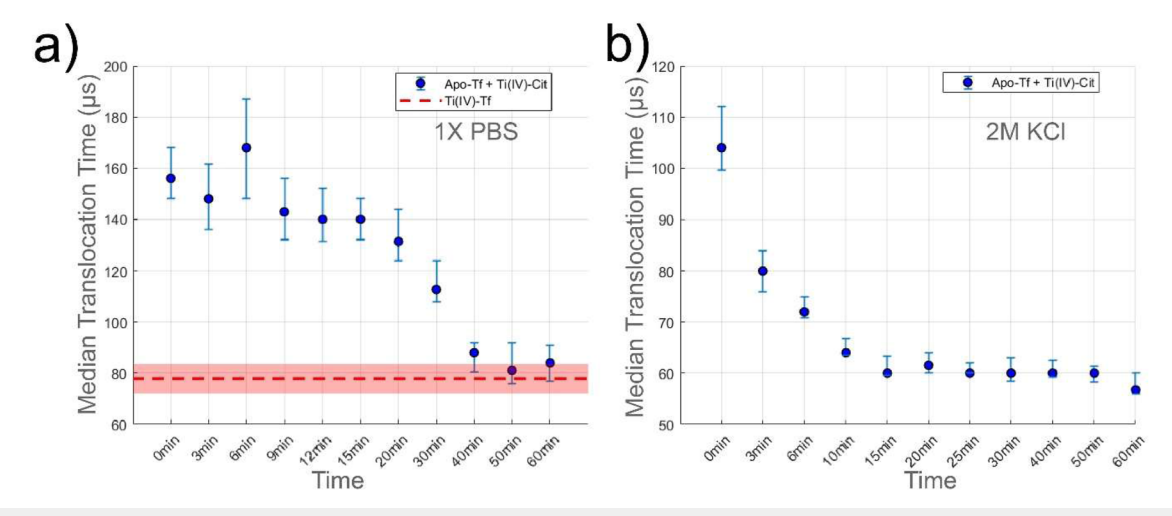


FIG. 4. Real-time monitoring of the binding between Ti(IV) and apo-transferrin using a nanopore. The median translocation times decrease upon the addition of the Ti(IV)-citrate species, which binds to apo-transferrin. The median translocation times were measured at regular time intervals in (a) 1X PBS and (b) 2M KCI. The error bars represent the bootstrapped confidence intervals on the medians. The red dotted line in (a) represents the median translocation time of Ti(IV)-transferrin.

After a certain time duration, the reaction reaches a steady state, where the median translocation time no longer changes with time. This transition suggests that the reaction has completed (reached equilibrium), with the majority of the apo-transferrin molecules transformed into Ti(IV)-transferrin. This demonstration highlights the potential of a nanopore as an affordable, single-molecule, and label-free method for real-time monitoring of the progression of a biochemical reaction. The purpose of this experiment was to establish the feasibility of using a nanopore as a real-time monitor of a biochemical reaction. Consequently, we added an excess of the reacting ligand [titanium(IV) citrate]. For precise reaction curves, the exact concentration of the reacting ligand would need to be determined. In future experiments, we can ascertain the precise concentration of titanium(IV) citrate to obtain more accurate reaction data.

### IV. CONCLUSION

We employed a solid-state nanopore to monitor the binding of Ti(IV) to transferrin in a single-molecule, real-time fashion. Our observations revealed that Ti(IV)-bound transferrin translocated across the nanopore more rapidly than Ti(IV)-free transferrin, enabling their differentiation from one another. We attribute this difference in translocation time to the more compact and stable conformation adopted by Ti(IV)-transferrin compared to the more unfolded conformation of apo-transferrin. It is well documented that apo-transferrin is less stable than metal-ion-bound transferrin and tends to adopt a more unfolded state. In future experiments, we aim to determine the exact quantity of reacting ligands to obtain precise reaction curves.

### SUPPLEMENTARY MATERIAL

The supplementary material contains IV plots of all the nanopores used during experiments. It also contains the results of nanopore experiments carried out with a 100 kHZ low-pass Bessel filter and a control experiment where holo-transferrin (iron-containing) is also analyzed.

#### **ACKNOWLEDGMENTS**

This work was supported by the National Science Foundation (Grant No. CBET #2022374), the Ministry of Education of the Republic of Korea, and the National Research Foundation of Korea (Grant No. RS-2023-00259957). The authors would also like to thank Professor Ann M. Valentine at Temple University for her selfless and invaluable guidance and support in the synthesis of Ti(IV)-transferrin and its characterization using UV-vis spectroscopy. The authors also thank Professor Kytai Nguyen and Ankitha Srinivasa at the University of Texas at Arlington for their generous support in measuring the zeta potential of the proteins used during experiments.

### **AUTHOR DECLARATIONS**

### **Conflict of Interest**

The authors have no conflicts to disclose.

#### **Author Contributions**

Matthew O'Donohue: Conceptualization (equal); Formal analysis (equal); Methodology (equal); Visualization (equal); Writing – original draft (equal); Writing – review & editing (equal). Madhav L. Ghimire: Conceptualization (supporting); Methodology (supporting); Writing – review & editing (supporting). Sangyoup Lee: Conceptualization (supporting); Funding acquisition (supporting); Writing – review & editing (supporting). Min Jun Kim: Conceptualization (equal); Funding acquisition (equal); Investigation (equal); Writing – review & editing (equal).

### **DATA AVAILABILITY**

The data that support the findings of this study are available from the corresponding author upon reasonable request.

### **REFERENCES**

- <sup>1</sup>N. Abbaspour, R. Hurrell, and R. Kelishadi, "Review on iron and its importance for human health," J. Res. Med. Sci. **19**(2), 164 (2014); available at https://www.ncbi.nlm.nih.gov/pmc/articles/PMC3999603/
- <sup>2</sup>R. J. Wood et al., Modern Nutrition in Health and Disease, Lippincott's Illustrated Reviews Biochemistry (Lippincott Williams & Wilkins, 2005), pp. 248–270.
- <sup>3</sup>L. R. McDowell, *Minerals in Animal and Human Nutrition* (Academic Press, Inc., 1992).
- <sup>4</sup>R. Yip and P. R. Dallman, in *Iron: Present Knowledge in Nutrition*, edited by B. A. Bowman and R. M. Russell (Springer, 1996), pp. 311–328.
- <sup>5</sup>H. A. Huebers and C. A. Finch, "The physiology of transferrin and transferrin receptors," Physiol. Rev. **67**(2), 520–582 (1987).
- <sup>6</sup>P. Aisen and E. B. Brown, "Structure and function of transferrin," Prog. Hematol. **9**, 25–56 (1975); available at https://pubmed.ncbi.nlm.nih.gov/766075/
- <sup>7</sup>H. A. Huebers and C. A. Finch, "Transferrin: Physiologic behavior and clinical implications," Blood **64**, 763–767 (1984).
- <sup>8</sup>C.-B. Laurell and B. Ingelman, "The iron-binding protein of swine serum," Nutr. Rev. 43(7), 209–211 (1985).
- <sup>9</sup> A. D. Tinoco and A. M. Valentine, "Ti(IV) binds to human serum transferrin more tightly than does Fe(III)," J. Am. Chem. Soc. **127**(32), 11218–11219 (2005).
- <sup>10</sup>R. B. Martin *et al.*, "Transferrin binding of Al<sub>3</sub> and Fe<sub>3</sub> ," Clin. Chem. **33**, 405 (1987); available at https://pubmed.ncbi.nlm.nih.gov/3815806/
- <sup>11</sup>H. Brock, "Transferrins," in *Metalloproteins*, *Part 2*, edited by P. M. Harrison (Verlag Chemie, Weinheim, 1995), pp. 183–261.
- <sup>12</sup>H. Sun *et al.*, "The first specific TiIV-protein complex: Potential relevance to anticancer activity of titanocenes," Angew. Chem., Int. Ed. 37(11), 1577–1579 (1998)
- <sup>13</sup>J. C. Cannon and N. D. Chasteen, "Nonequivalence of the metal binding sites in vanadyl-labeled human serum transferrin," Biochemistry 14(21), 4573–4577 (1975).
- <sup>14</sup>P. Aisen, R. Aasa, and A. G. Redfield, "The chromium, manganese, and cobalt complexes of transferrin," J. Biol. Chem. 244(17), 4628–4633 (1969).
- <sup>15</sup>J. B. Vincent and S. Love, "The binding and transport of alternative metals by transferrin," Biochim. Biophys. Acta, Gen. Subj. 1820(3), 362–378 (2012).
- <sup>16</sup>J. P. Curtin *et al.*, "The role of citrate, lactate and transferrin in determining titanium release from surgical devices into human serum," JBIC, J. Biol. Inorg. Chem. 23, 471–480 (2018).
- <sup>17</sup>L. Ciavatta *et al.*, "On the hydrolysis of the titanium(IV) ion in chloride media," Polyhedron 4(1), 15–22 (1985).
- <sup>18</sup> A. E. Martell and R. M. Smith, *Critical Stability Constants* (Plenum Press, New York, 1974), Vol. 1.
- <sup>19</sup>L. Xue *et al.*, "Solid-state nanopore sensors," Nat. Rev. Mater. **5**(12), 931–951
- <sup>20</sup>Y. Luo et al., "Application of solid-state nanopore in protein detection," Int. J. Mol. Sci. 21(8), 2808 (2020).

- <sup>21</sup> M. O'Donohue *et al.*, "Use of a solid-state nanopore for profiling the transferrin receptor protein and distinguishing between transferrin receptor and its ligand protein," Electrophoresis **44**(1–2), 349–359 (2023).
- <sup>22</sup>J. Sha *et al.*, "Identification of spherical and nonspherical proteins by a solid-state nanopore," Anal. Chem. **90**(23), 13826–13831 (2018).
- <sup>23</sup>F. Piguet *et al.*, "Identification of single amino acid differences in uniformly charged homopolymeric peptides with aerolysin nanopore," Nat. Commun. **9**(1), 966 (2018)
- <sup>24</sup>P. Martin-Baniandres *et al.*, "Enzyme-less nanopore detection of post-translational modifications within long polypeptides," Nat. Nanotechnol. **18**, 1335 (2023).
- <sup>25</sup>J. Saharia *et al.*, "Molecular-level profiling of human serum transferrin protein through assessment of nanopore-based electrical and chemical responsiveness," ACS Nano **13**(4), 4246–4254 (2019).
- <sup>26</sup> J. Saharia *et al.*, "Modulation of electrophoresis, electroosmosis and diffusion for electrical transport of proteins through a solid-state nanopore," RSC Adv. **11**(39), 24398–24409 (2021).
- <sup>27</sup>J. Saharia, Y. M. Nuwan, D. Y. Bandara, and M. J. Kim, "Investigating protein translocation in the presence of an electrolyte concentration gradient across a solid-state nanopore," Electrophoresis 43(5–6), 785–792 (2022).
- <sup>28</sup>K. J. Freedman *et al.*, "Solid-state nanopore detection of protein complexes: Applications in healthcare and protein kinetics," Small **9**(5), 750–759 (2013).
- <sup>29</sup> K. J. Freedman *et al.*, "Single molecule unfolding and stretching of protein domains inside a solid-state nanopore by electric field," Sci. Rep. 3(1), 1638 (2013).
- <sup>30</sup>K. J. Freedman *et al.*, "Nonequilibrium capture rates induce protein accumulation and enhanced adsorption to solid-state nanopores," ACS Nano **8**(12), 12238–12249 (2014).
- <sup>31</sup> K. J. Freedman *et al.*, "Chemical, thermal, and electric field induced unfolding of single protein molecules studied using nanopores," Anal. Chem. **83**(13), 5137–5144 (2011).
- <sup>32</sup>J. Saharia *et al.*, "Assessment of 1/f noise associated with nanopores fabricated through chemically tuned controlled dielectric breakdown," Electrophoresis **42**(7–8), 899–909 (2021).
- <sup>33</sup> J. Saharia *et al.*, "Over one million DNA and protein events through ultra-stable chemically-tuned solid-state nanopores," Small **19**, 2300198 (2023).

- <sup>34</sup>Y. M. Nuwan, D. Y. Bandara *et al.*, "Beyond nanopore sizing: Improving solid-state single-molecule sensing performance, lifetime, and analyte scope for omics by targeting surface chemistry during fabrication," Nanotechnology **31**(33), 335707 (2020).
- <sup>35</sup>H. Kwok, K. Briggs, and V. Tabard-Cossa, "Nanopore fabrication by controlled dielectric breakdown," PLoS One **9**(3), e92880 (2014).
- <sup>36</sup>J. M. Collins *et al.*, "Titanium(IV) citrate speciation and structure under environmentally and biologically relevant conditions," Inorg. Chem. **44**(10), 3431–3440 (2005).
- <sup>37</sup>Y. F. Deng *et al.*, "Speciation of water-soluble titanium citrate: Synthesis, structural, spectroscopic properties and biological relevance," Polyhedron **26**(8), 1561–1569 (2007).
- <sup>38</sup>Y. M. Bandara, D. Y. Nuwan *et al.*, "Nanopore data analysis: Baseline construction and abrupt change-based multilevel fitting," Anal. Chem. **93**(34), 11710–11718 (2021).
- <sup>39</sup>B. Ledden et al., Nanopores: Sensing and Fundamental Biological Interactions (Springer, 2011), pp. 129–150.
- $^{40}$  A. A. Rashin, M. Iofin, and B. Honig, "Internal cavities and buried waters in globular proteins," Biochemistry 25(12), 3619–3625 (1986).
- <sup>41</sup>R. Phillips et al., Physical Biology of the Cell (Garland Science, 2012).
- $^{42}$ W. Si and A. Aksimentiev, "Nanopore sensing of protein folding," ACS Nano 11(7), 7091-7100 (2017).
- <sup>43</sup>W. B. Dunbar, "Comment on accurate data process for nanopore analysis," Anal. Chem. 87(20), 10650–10652 (2015).
- $^{44}\mathrm{C}$  . Wen, D. Dematties, and S.-L. Zhang, "A guide to signal processing algorithms for nanopore sensors," ACS Sens. **6**(10), 3536–3555 (2021).
- <sup>45</sup>D. Rodriguez-Larrea and H. Bayley, "Multistep protein unfolding during nanopore translocation," Nat. Nanotechnol. 8(4), 288–295 (2013).
- <sup>46</sup>C. Merstorf *et al.*, "Wild type, mutant protein unfolding and phase transition detected by single-nanopore recording," ACS Chem. Biol. 7(4), 652–658 (2012).
- <sup>47</sup>A. Asandei *et al.*, "Nanoscale investigation of generation 1 PAMAM dendrimers interaction with a protein nanopore," Sci. Rep. 7(1), 6167 (2017).
- $^{48}$ E. C. Yusko *et al.*, "Single-particle characterization of A $\beta$  oligomers in solution," ACS Nano 6(7), 5909–5919 (2012).
- <sup>49</sup>L. Mereuta *et al.*, "Protein nanopore-based, single-molecule exploration of copper binding to an antimicrobial-derived, histidine-containing chimera peptide," Langmuir 28, 17079–17091 (2012).